Bioorganic & Medicinal Chemistry xxx (2018) xxx–xxx

Contents lists available at ScienceDirect

Bioorganic & Medicinal Chemistry

journal homepage: www.elsevier.com/locate/bmc

Building bridges for highly selective, potent and stable oxytocin and vasopressin analogs

Rhiannon Beard [a], Andy Stucki [b], Muriel Schmitt [b], Gabrielle Py [b], Christophe Grundschober [b], Antony D. Gee [c], Edward W. Tate [a,*]

[a] Department of Chemistry, Imperial College London, Exhibition Road, London SW7 2AZ, UK
[b] Roche Pharma Research and Early Development, Discovery Neuroscience, Roche Innovation Center Basel, F. Hoffmann-La Roche Ltd, Grenzacherstrasse 124, 4070 Basel, Switzerland
[c] Division of Imaging Sciences, King's College London, 4th Floor, Lambeth Wing, St Thomas' Hospital, SE1 7EH London, UK

ARTICLE INFO

Article history:
Received 28 January 2018
Revised 9 March 2018
Accepted 10 March 2018
Available online xxxx

Keywords:
Oxytocin
Disulfide bridging
Cyclic peptides
Peptide-based drugs
Increased stability

ABSTRACT

Oxytocin (OT) is an exciting potential therapeutic agent, but it is highly sensitive to modification and suffers extensive degradation at elevated temperature and *in vivo*. Here we report studies towards OT analogs with favorable selectivity, affinity and potency towards the oxytocin receptor (OTR), in addition to improving stability of the peptide by bridging the disulfide region with substituted dibromo-xylene analogs. We found a sensitive structure-activity relationship in which meta-cyclized analogs (dOT_{meta}) gave highest affinity (50 nM K_i), selectivity (34-fold), and agonist potency (34 nM EC_{50}, 87-fold selectivity) towards OTR. Surprisingly, ortho-cyclized analogs demonstrated OTR and vasopressin V_{1a} receptor subtype affinity (220 nM and 69 nM, respectively) and pharmacological activity (294 nM and 35 nM, respectively). V_{1a} binding and selectivity for ortho-cyclized peptides could be improved 6-fold by substituting a neutral residue at position 8 with a basic amino acid, providing potent antagonists (14 nM IC_{50}) that displayed no activation of the OTR. Furthermore, xylene-bridged analogs demonstrated increased stability compared to OT at elevated temperature, demonstrating promising therapeutic potential for these analogs which warrants further study.

1. Introduction

Oxytocin (OT), a nonapeptide released from the pituitary gland, is a promising therapeutic agent that is heavily involved with lactation and uterine contraction in the peripheral system and is further linked with complex neurological disorders in the central nervous system. For example, OT is the World Health Organization's recommended drug to prevent postpartum hemorrhaging, which is one of the most common causes of maternal morbidity.[1,2] However, OT suffers from limited stability in aqueous solution that is especially problematic in subtropical climates where the majority of maternal deaths occur.[3–6] Further, OT is highly susceptible to metabolic degradation, having an *in vivo* half-life of 3 min, causing substantial loss of activity.[7]

Common approaches to overcome peptide degradation, including use of unnatural and D-amino acids, terminal capping and chemical modification or mutation of the proteolytic recognition sites, are often unsuitable for OT since its biological activity is highly sensitive to structural change. This is because OT shares a molecular structure closely related to vasopressin (also known as arginine vasopressin, AVP), making the development of a highly specific and stable oxytocin receptor (OTR) ligand challenging. Both OT and AVP contain a disulfide bridge between residues 1 and 6, resulting in a structure containing a cyclic core comprising six amino acids with a flexible three-residue amidated tail (Fig. 1, Table 1). The peptides differ by the amino acids at position 3, and at position 8 whereby OT-related peptides contain a neutral residue, while AVP peptides bear a basic amino acid. This subtle difference in polarity at position 8 is thought to confer the molecules' interaction with its receptor that, in turn, is related to its distinctive function.[8,9] However, due to their common structure, OT and AVP peptides bind to and act on multiple members of the G-protein coupled receptor family to exert their pharmacological effects, including OTR, and AVP receptor subtypes V_{1a}, V_{1b} and V_2.[10] For OT, Tyr2 and Asn5 are fundamental for activity in the uterus while residues Leu8, Pro7, Gln4 and Ile3 are key for receptor binding.[11]

Specifically, to improve the stability of OT two main strategies have been used (i) *N*-terminal deamination,[12,13] and (ii) disulfide bond engineering, since the disulfide bond is generally not implicated in OTR binding or activity. In the case of disulfide

* Corresponding author.
E-mail address: e.tate@imperial.ac.uk (E.W. Tate).

https://doi.org/10.1016/j.bmc.2018.03.019
0968-0896/

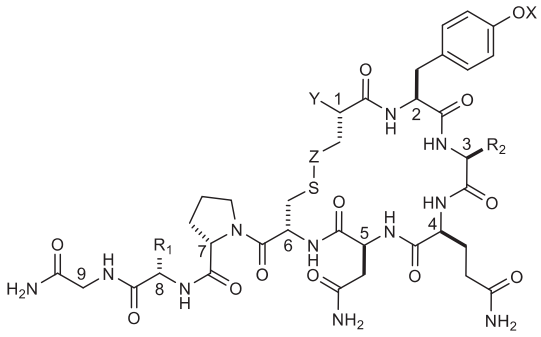

Fig. 1. Structure of therapeutic peptide OT, AVP and related analogs, with variables presented alongside in Table 1.

Table 1
Sequence residues for OT and related peptides.

Peptide	R_1	R_2	X	Y	Z
OT	Leu	Ile	H	NH_2	S
dOT	Leu	Ile	H	H	S
AVP	Arg	Phe	H	NH_2	S
dOT(L8R)	Arg	Ile	H	H	S
Carbetocin	Leu	Ile	CH_3	H	CH_2

engineering, a variety of modifications at this position have been investigated, typically replacing the disulfide bridge with alternatives including thioether,[14] carbon,[15,16] lactam,[17] and diselenide bridges.[18] Structure activity relationships (SARs) have identified that introduction of one alternative atom on the disulfide bond (such as selenium) causes a subtle change in the ring region of OT that is tolerated for OTR binding and efficacy,[15,19] while reductions in the ring size of OT can abolish OTR activity. However, the majority of studies omit determination of AVP receptor subtype activity, leaving a question over alterations in receptor selectivity induced by these chages.[19] Alternatively, carbetocin, an OT mimetic with an improved pharmacokinetic profile and prolonged uterotonic activity,[14] shows reduced selectivity and affinity towards the OTR (10-fold lower than OT), and is only a OTR partial agonist (Fig. 1).[20,21] In addition, recent reports have emerged that suggests carbetocin is also a V_{1a} and V_{1b} antagonist, complicating its pharmacological profile.[22]

In a complementary and relatively less studied approach to disulfide engineering, disulfide bridging represents an attractive alternative that circumvents the lengthy and complex synthesis of unnatural cyclized peptides through engineering strategies. For example, Collins et al. recently demonstrated that a maleimide-functionalized polymer could successfully bridge the disulfide region of OT, resulting in a conjugate with increased thermal stability.[23]

In the present study, we investigated the biological activity and stability of OT analogs bridged by dibromo-xylene molecules that offer an irreversible covalent modification. Previously, dibromoxylenes have been used to assist peptide cyclisation,[24] and increase proteolytic stability or helicity of peptides,[25,26] with further applications in the construction of protein mimics.[27] Furthermore, a range of substituted analogs are available commercially, enabling bridging distance structure-activity relationships (SAR) to be studied. We produced a library of cyclized OT analogs based on *N*-terminally deaminated OT (dOT), which has been reported to have increased stability compared to OT.[7] In addition, omission of a *N*-terminal amine on dOT prevented any complications from competing side reactions during cyclization. The peptide library was screened for binding affinity, biological activity and stability at elevated temperature using *in vitro* assays, revealing promising potency, selectivity and stability profiles driven by xylene-bridging in OT analogs.

2. Results and discussion

2.1. Synthesis of OT and peptide analogs

Native OT, deaminated OT (dOT) and dOT(L8R) were successfully synthesized *via* automated fluorenylmethoxycarbonyl (Fmoc) solid phase peptide synthesis (SPPS), and coupling with 2-(1*H*-benzotriazol-1-yl)-1,1,3,3-tetramethyluronium hexafluorophosphate (HBTU). In the case of dOT and dOT(L8R), a deaminated protected cysteine was made by reacting triphenylmethylchloride in dicholomethane with 3-mercaptopropionic acid[28], then coupled in the final position. Peptides were cleaved from the resin using trifluoroacetic acid (TFA) in the presence of 2.5% DTT to prevent oxidation of cysteine or deaminated cysteine residues. Crude peptides were purified by reverse phase (RP) liquid chromatography mass spectrometry (LC-MS) using either water/methanol or water/acetonitrile (MeCN). When required, cyclization of native disulfide bonds was achieved by stirring the peptide in ammonium bicarbonate buffer in the presence of oxygen for up to three days. Both purified peptides were lyophilized, and characterized by RP LC-MS (Supplementary Fig. 1.1), which is presented in Table 2.

2.2. Disulfide bridging of dOT with xylene analogs

Cyclization of dOT analogs using various isomers of dibromoxylene was first attempted in a mixture of ammonium bicarbonate and acetonitrile, at room temperature and at a final concentration of 1 mM peptide. While full conversion was seen after 10 min, a small proportion of polymerized product for both meta- (11%) and para- (21%) dibromoxylene-cyclized dOT was detected. Pleasingly, this side product was removed when the reaction was performed at higher dilution (0.5 mM) and lower dibromoxylene molar equivalents (1.1 equivalents vs. 3 equivalents), affording all peptides efficiently and in good overall yield (Table 2, Fig. 2). Xylene-bridged analogs showed reduced solubility in water; addition of 15% v/v DMSO solved this issue.

2.3. Binding affinity of peptides against OTR and AVP receptor subtypes

The OTR has a substantial reliance on cholesterol for proper functioning that has, in turn, presented severe challenges to attempts to generate a crystal structure of the OT-OTR complex.[29] Further, common problems facing solubilized OTR include reductions in affinity and loss of characteristic binding properties towards ligands. Therefore, SAR for OT analogs is best determined using *in vitro* receptor binding studies, with conclusive studies also testing against AVP receptor subtypes to address selectivity. Inhibitory constant (K_i) values for human receptors are presented in Table 3. Displacement of either [^{3}H]OT or [^{3}H]AVP by dOT analogs was measured over a concentration range of 0.95–30000 nM, while non-specific binding of peptide analogs was defined using the appropriate cold endogenous peptide.[30] Receptor specificity was calculated by comparing the affinity of ligands to members of the OT and the AVP receptor family member that demonstrated the highest binding capacity.

While all analogs screened suffered a decrease in binding affinity toward the OTR compared to native OT, selectivity over the AVP receptor subtypes was improved for dOT_{meta} and maintained for the dOT_{para} derivative (Table 3, Fig. 3a). Further, meta-cyclization demonstrated the highest affinity for OTR binding among the analogs tested. Interestingly, dOT_{ortho} showed high affinity and preferential binding towards V_{1a} receptor (Fig. 3b). The introduction of a

Table 2
Characterization data and yields for OT peptide analogs.

Peptide	MW (Da)	Rt (min)	ES peaks (*m*/*z*)	Yield (%)[c]
OT_{cy}	1006.4	9.64[a]	1007.90 (m + 1)	18
dOT_{oc}	993.4	11.82[a]	994.72 (m + 1)	21
dOT_{cy}	991.4	11.74[a]	992.61 (m + 1)	17
$dOT(L8R)_{oc}$	1037.2	9.71[a]	1038.67 (m + 1)	24
dOT_{meta}	1095.5	14.19[a]	1096.67 (m + 1)	16
dOT_{para}	1095.5	14.24[a]	1096.67 (m + 1)	16
dOT_{ortho}	1095.5	14.05[a]	1096.67 (m + 1)	18
$dOT(L8R)_{ortho}$	1139.4	8.72[b]	1140.48 (m + 1)	20

Key: d = deaminated; cy = cyclized; oc = open chain; meta = meta-xylene bridged; para = para-xylene bridged; ortho = ortho-xylene bridged.
[a] LCMS analytical Method 1 used to analyze peptide (please refer to Experimental Section 4.4 for details).
[b] LCMS analytical Method 2 used to analyze peptide.
[c] Yields are calculated based on resin load.

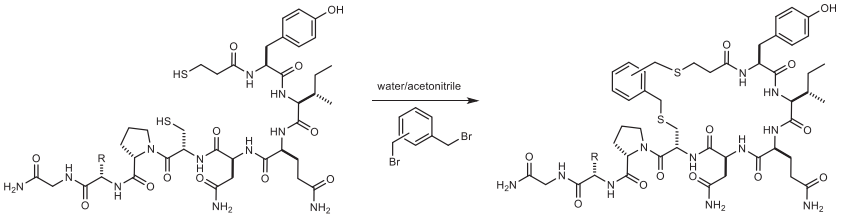

Fig. 2. Conjugation reaction with substituted dibromo-xylene reagents to form disulfide bridged analogs.

Table 3
Peptide inhibition constants (K_i in nM) and selectivity profile.

K_i (nM)					Receptor selectivity	
Peptide	OTR	V_{1a}	V_{1b}	V_2	OTR[a]	V_{1a}[b]
OT	1.2 ± 0.3	20 ± 3	>6000	>6000	17	0.06
AVP	6 ± 1	2 ± 0.3	2 ± 0.6	32 ± 4	0.3	3.0
dOT_{meta}	50 ± 14	1681 ± 13	>6000	>6000	34	0.03
dOT_{para}	142 ± 12	1954 ± 8	>6000	>6000	14	0.07
dOT_{ortho}	220 ± 10	69 ± 12	>6000	>6000	0.3	3.2
$dOT(L8R)_{ortho}$	166 ± 19	30 ± 6	>6000	>6000	0.2	5.5

Binding of OT, AVP and xylene-bridged analogs to human OT/AVP receptor subtypes. Values are the mean value of three different experiments, each performed in duplicate.
[a] Calculated by dividing strongest AVP receptor subtype binding value with OTR value.
[b] Calculated by dividing OTR binding value with V_{1a} value.

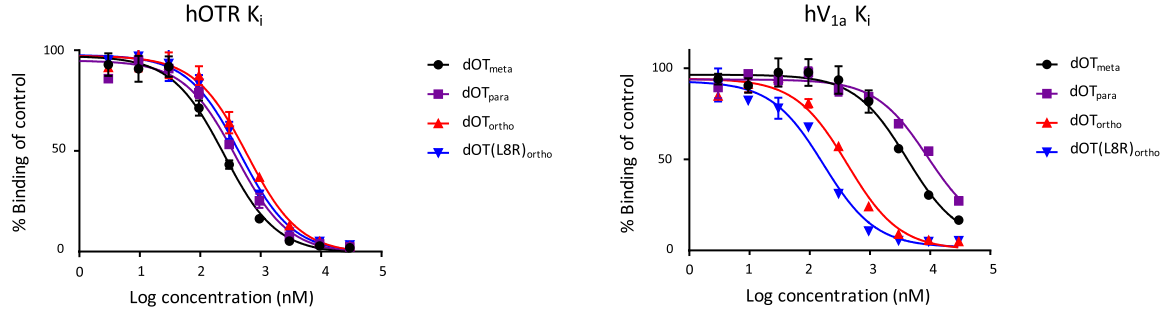

Fig. 3. Binding of xylene-bridged dOT analogs to human OTR or V_{1a} receptor subtypes measured in a competition binding assay.

basic residue at position 8 further enhanced the affinity and selectivity profile for analog $dOT(L8R)_{ortho}$ towards V_{1a} receptor compared to both dOT_{ortho} and AVP.

2.4. Biological activity of peptides by calcium flux assay

OT/AVP peptides exert their biological function through binding to the relevant receptor, causing a measurable increase in intracellular Ca^{2+} in a fluorescence assay.[29,30] Half-maximal effective concentration (EC_{50}) values or functional antagonism (half-maximal inhibitory concentration, IC_{50}) for the peptide series is reported in Table 4. In addition to receptor binding, dOT_{meta} and dOT_{para} showed excellent agonist potency (EC_{50}) and selectivity towards OTR. In agreement with affinity measurements, dOT_{meta} was the most potent and selective OTR agonist, however maximal activation was 75 ± 1%, suggesting that dOT_{meta} is a partial agonist (Fig. 4a), but nevertheless more effective than carbetocin (45 ± 6%).[22] Surprisingly, dOT_{ortho} showed agonist activity towards OTR

Table 4
Peptide agonist (EC_{50} in nM), antagonist (IC_{50} in nM) and selectivity profile.

	Agonist; EC_{50}				Receptor selectivity	
Peptide	OTR	V_{1a}	V_{1b}	V_2	OTR[a]	V_{1a}[b]
OT	0.3 ± 0.1	9 ± 2	33 ± 7	29 ± 5	30	0.03
dOT_{meta}	34 ± 6	>20000	2966 ± 120	3900 ± 350	87	–
dOT_{para}	109 ± 24	>20000	2223 ± 533	3669 ± 146	20	–
dOT_{ortho}	294 ± 58	>20000	8302 ± 1982	10764 ± 101	28	–
$dOT(L8R)_{ortho}$	>10000	>20000	9263 ± 957	18919 ± 146	–	–

	Antagonist; IC_{50}				Receptor selectivity	
Peptide	OTR	V_{1a}	V_{1b}	V_2	OTR	V_{1a}
dOT_{meta}	Agonist	4400	Agonist	Agonist	–	–
dOT_{para}	Agonist	7862	Agonist	Agonist	–	–
dOT_{ortho}	Agonist	35 ± 28	Agonist	Agonist	–	8.4[c]
$dOT(L8R)_{ortho}$	1724 ± 177	14 ± 8	Agonist	Agonist	0.008	123

[a] Calculated by dividing strongest AVP receptor subtype binding value with OTR value.
[b] Calculated by dividing OTR subtype agonist value with V_{1a} antagonist value.
[c] Calculated by dividing OTR subtype binding value with V_{1a} value.

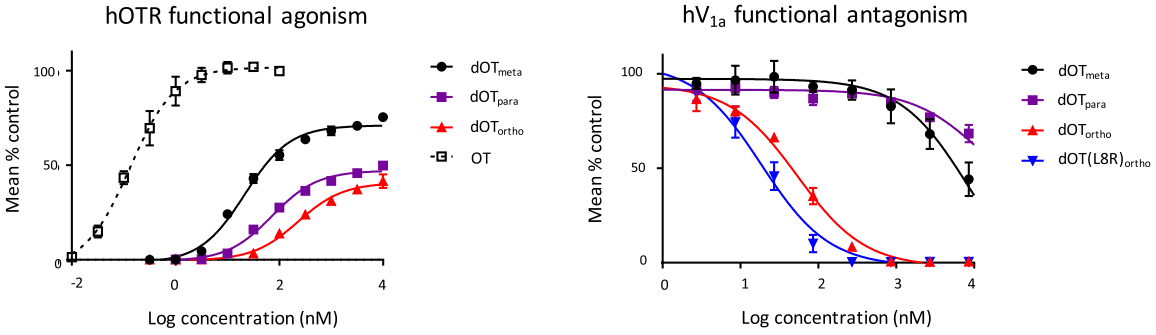

Fig. 4. Function agonism or antagonism of xylene-bridged dOT analogs to human OTR or V_{1a} receptor subtypes measured in a competition assay.

and antagonist activity towards V_{1a} receptor. This phenomenon has been shown recently for carbetocin, which displays agonistic behavior towards OTR and antagonism towards the V_{1a} and V_{1b} receptors.[22] Alternatively, a complete switch in receptor selectivity was demonstrated for analog $dOT(L8R)_{ortho}$ that displayed potent antagonist activity and selectivity towards the V_{1a} receptor (Fig. 4b), showing no activation of OTR.

We demonstrate here that dOT_{meta} is a selective human OTR agonist with no antagonist activity towards the OTR detected, while $dOT(L8R)_{ortho}$ was identified as a selective V_{1a} receptor antagonist. Whilst these data demonstrate that high affinity and selective binders can be achieved through disulfide bridging, modification to the OT backbone significantly influences affinity, selectivity and potency. The sensitivity of OT to alterations in ring size emphasizes the importance of screening multiple receptor subtypes when exploring OT ring modifications due to the complex pharmacological profile of this hormone. We hypothesize that modification of the disulfide bond distorts the cyclic region of these analogs, which influences their interaction with OT/AVP receptor subtypes.

Pharmacology profile of OT, AVP and xylene-bridged analogs to human OT/AVP receptor subtypes. Values are the mean value of three different experiments, each performed in duplicate.

2.5. Thermal stability

The formation of a non-reversible covalent linkage in place of a disulfide bond is expected to improve the stability of OT analogs since previous research suggests that reactions involving this region plays a central role for OT degradation, being prone to oxidation, dimerization, and β-elimination.[6] Peptide stability was

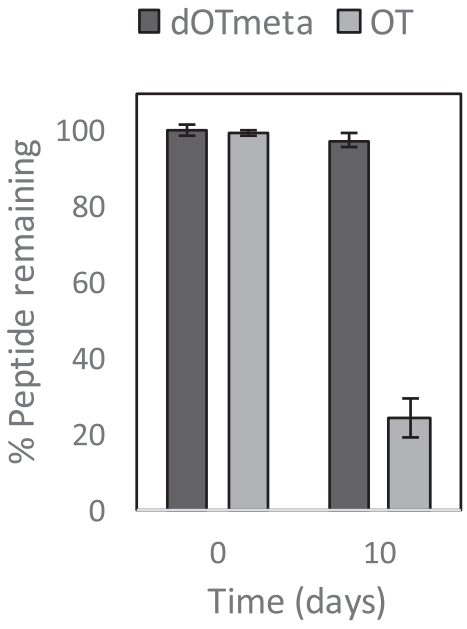

Fig. 5. Degradation of aqueous solutions of native OT and dOT_{meta} conjugates at 50 °C.

investigated through an accelerated stability test in which dOT_{meta} was compared to OT, as a representative analog of the bridged peptides. Peptides were dissolved in water to a concentration of 0.5 mg mL^{-1} and heated to 50 °C in a heat block for 10 days. After this time aliquots were removed and analysed by RP-LCMS. The amount of remaining peptide was calculated as a percentage of the relevant peak remaining before heat exposure. In this study, degradation was prevented by conjugation of dibromo-xylene (Fig. 5).

3. Conclusions

We report rapid and effective synthesis of xylene-bridged analogs of dOT and determined the impact on biological activity and stability following modification. This flexible approach facilitated access to a variety of isomeric xylene bridges, which led to diverse modulation of receptor selectivity, potency and affinity, presenting an alternative pharmacological profile and therapeutic potential to OT. A key finding from this work was that ring size and geometry influenced OTR binding, with meta-bridged analogs demonstrating the most favorable binding and pharmacology profile towards OTR. dOT_{meta} demonstrated an improved selectivity profile for both binding and activation towards the OTR and showed minimal V_{1a} antagonist activity, a more selective pharmacological than the widely used drug carbetocin.[22,31] It was surprising that dOT_{ortho} displayed preferential binding affinity and selectivity towards V_{1a}, which can function as both a OTR agonist and V_{1a} antagonist, which could be further enhanced for $dOT(L8R)_{ortho}$, incorporating a basic residue at position 8, a mutation important for AVP receptor engagement. Notably, $dOT(L8R)_{ortho}$ displayed improved binding selectivity towards V_{1a} over AVP, with substantial antagonist activity only towards this receptor subtype.

OT binds and activates OTR, V_{1a} and V_{1b} receptor subtypes, which has contributed to limited or debated efficacy in clinical practice.[32,33] The molecules reported here have a defined binding and pharmacology profile, making them potentially useful tools for probing the pharmacological potential of OTR. Furthermore, xylene-bridging proved useful in enhancing thermal stability, demonstrating minimal degradation compared to native OT at elevated temperatures. Consequently, the xylene bridged analogs represent an interesting modification to OT with increased stability, worthy of further investigation.

4. Experimental

4.1. Materials

General laboratory chemicals, were obtained from Sigma-Aldrich Chemical Co. and used without further purification. Rink amide Tentagel resin (0.71 mmol/g) was obtained from Rapp Polymere while *N*,*N*-dimethylformamide (DMF), *N*-Methyl-2-pyrrolidone (NMP), piperidine and trifluoroacetic acid (TFA) were obtained from Merck Millipore. Fmoc (Fluorenylmethoxycarbonyl)-l-amino acids, HBTU, *N*,*N*-Diisopropylethylamine (DIPEA) were purchased from AGTC bioproducts. Gases were from BOC. Solutions and buffers were prepared with Ultra-pure water obtained from a Millipore Elix Q-guard purification system.

4.2. Equipment

Peptides were purified and analysed on a Waters LC-MS system consisting of i) Waters 2767 autosampler for samples injection and collection; ii) Waters 515 HPLC pump to deliver the mobile phase to the source; iii) Waters 3100 mass spectrometer with ESI; and, iv) Waters 2998 Photodiode Array (detection at 200–600 nm)), equipped with XBridge C_{18} reverse-phase columns with dimensions 4.6 mm × 100 mm for analytical and 19 mm × 100 mm for preparative runs. Solvents were degassed with helium and supplemented with 0.1% formic acid prior to use.

4.3. Solid phase peptide synthesis

Peptides were synthesised using automated solid-phase peptide synthesis with Rink amide Tentagel resin on a ResPep SL apparatus (Intavis) using the supplied Multipep software. Synthesis was carried out in peptide synthesis grade DMF. Resin (20 μmol/well) was swelled in DMF for 30 min before synthesis. Subsequent steps were conducted automatically. *N*-α-amino Fmoc groups were deprotected using 20% (v/v) piperidine in DMF (400 μL, 2 × 5 min). The Fmoc-protected amino acid (100 μmol, 5.0 eq.; 200 μL of 0.5 M stock solution in NMP) for coupling was pre-activated with HBTU (95 μmol, 4.75 eq.; 190 μL of 0.5 M stock solution in NMP) and NMM (200 μmol, 10 eq.; 50 μL of 4 M stock solution in NMP). Coupling was allowed to take place over 30–55 min and amino acids were 'double-coupled' (i.e. the coupling step was repeated). To prevent deletion sequences, any unreacted *N*-terminal amines were acetylated with 'capping mixture' (400 μL of 5% (v/v) Ac_2O in DMF) for 10 min. The resin was washed with DMF (3 × 1 mL) between the deprotection, coupling and acylation steps. The typical cycle was repeated until the final (*N*-terminal) amino acid coupling, when *N*-α-Fmoc deprotection at the final residue undertaken under usual conditions. Following synthesis, peptides were washed several times (3 × 1 mL DMF, 3 × 1 mL DCM, 3 × 1 mL MeOH, 3 × 1 mL Et_2O) and dried overnight in a desiccator. For the deprotection and cleavage of all peptides, a mixture of 1.5 mL TFA:H_2O:DTT:TIS (94:2.5:2.5:1) was added to resin bound peptide for 3 h. Crude peptides were precipitated using ice cold TBME, centrifuged at 4000 rpm for 15 min at 4 °C, and the supernatant discarded. The remaining peptides were washed with a fresh aliquot of TBME and the process repeated. Precipitate was dried in a desiccator over silica gel to yield off white solids which were dissolved in a H_2O:MeOH mixture for purification by RP LC-MS. Following purification, fractions containing pure peptide were combined and concentrated in the Genevac. Subsequently, pure peptides were re-dissolved in water and freeze-dried overnight.

4.4. Purification and characterization

LC-MS Analytical gradient 1: 5–98% MeOH in H_2O over 10 min, 98% MeOH was held for 2 min, MeOH was reduced from 98% to 5% over 1 min, and held at 5% until 18 min. *LC-MS Analytical gradient 2:* 5–98% MeCN in H_2O over 10 min, 98% MeCN was held for 2 min, MeCN was reduced from 98% to 5% over 1 min, and held at 5% until 18 min. *LC-MS semi-preparative gradient:* 5–25% MeOH in H_2O over 1 min, then increased to 75% MeOH over 10 min. MeOH was further increased to 98% over 1 min, held at 98% MeOH for 1 min, then reduced to 5% MeOH over 1 min where it was held for 4 min (18 min total).

4.5. Peptide modification

4.5.1. S-S disulfide bridging

Cyclization between internal cysteine residues was mediated in ammonium bicarbonate buffer (0.1 M, pH 8) at a final peptide concentration of 0.1 mg/mL. The solution was stirred for up to 3 days in the presence of oxygen at room temperature, after which time the solution was concentrated then lyophilized to yield pure peptide.

4.5.2. Xylene bridging of cysteine residues

A solution of dibromo-xylene (1.1 eq.; 0.55 mL from a 10 mM stock in MeCN) was added dropwise to a solution of dOT peptide in a mixture of ammonium bicarbonate (0.02 M, pH 7.8) and MeCN (3:1 respectively), affording an overall peptide concentration of 0.5 mg/ml. The resulting solution was agitated at room temperature for 30 min, and peptide products were purified and stored as a solution of water with 15% v/v DMSO.

4.6. Stability studies

Peptides were dissolved in water to a concentration of 0.5 mg mL^{-1} and incubated at 50 °C. Aliquots of the samples were removed after 10 days and analysed after direct injection (2 × 20 μL injection) by LC-MS.

4.7. In vitro studies

4.7.1. Membrane preparation

Human receptors were cloned by RT-PCR from total human liver RNA (V_{1a}), kidney RNA (V_2), or mammary gland RNA (OTR). Cell membranes were prepared from HEK293 cells transiently transfected with expression vector coding for human V_{1a}, human V_2, or mouse V_{1a}. For human OTR membrane preparation, a stable HEK clone expressing the receptor was selected. The transient or stable cells were grown in 20 L fermenters. For each receptor, 50 g of cell pellet was resuspended in 30 mL of ice cold lysis buffer (50 mM HEPES, 1 mM EDTA, and 10 mM $MgCl_2$ adjusted to pH 7.4, with the addition of complete cocktail of protease inhibitor (Roche Diagnostics) and homogenised with Polytron for 1 min. The preparation was centrifuged 20 min at 500 g at 4 °C, the pellet discarded, and the supernatant centrifuged for 1 h at 43,000 g at 4 °C (19,000 rpm). The pellet was resuspended in lysis buffer and sucrose (10%). The protein concentration was determined by the Bradford method and aliquots stored at −80 °C until use.

4.7.2. Binding affinity measurement

For vasopressin receptor binding studies, 60 mg of yttrium silicate SPA beads (Amersham) were mixed with an aliquot of membrane in binding buffer (50 mM Tris, 120 mM NaCl, 5 mM KCl, 2 mM $CaCl_2$, and 10 mM $MgCl_2$) for 15 min with mixing. 50 μL of bead/membrane mixture was then added to each well of a 96 well plate, followed by 50 μL of 4 nM ^{3}H-AVP (American Radiolabeled Chemicals). For total binding measurements, 100 μL of binding buffer was added to the respective wells; for nonspecific binding, 100 μL of 8.4 mM cold vasopressin or cold oxytocin for hOTR was added; and for compound testing, 100 μL of a serial dilution of each compound in 2% DMSO was added. The plate was incubated for 1 h at room temperature, centrifuged 1 min at 1000 g, and counted on a Packard Top-Count.

Binding to human OTR was measured by filtration binding using 1 nM ^{3}H-OT final concentration in 50 mM Tris, 5 mM $MgCl_2$, and 0.1% BSA (pH 7.4) buffer containing membranes. After compound addition as described above and 1 h of incubation at room temperature, the binding was terminated by rapid filtration under vacuum through GF/C filters, presoaked for 5 min with assay buffer, and washed 5 times with ice-cold assay buffer before counting. Non-specific binding counts were subtracted from each well and data normalized to the maximum specific binding set at 100%. K_i values were calculated using the Cheng-Prussoff equation. Saturation binding experiments performed for each assay indicated that a single homogeneous population of binding sites was being labeled. For receptor binding affinity (K_i) determination, compounds were tested at least 3 times in duplicate.

4.7.3. Stable cell culture and calcium flux assay using fluorescent imaging

CHO cells were stably transfected with expression plasmids encoding one of the human receptor of interest and grown in F-12 K, containing 10% fetal bovine serum, 1% penicillin-streptomycin, 1% L- glutamate, and 200 μg/mL geneticin at 37 °C in a 10% CO_2 incubator at 95% humidity. Cells were plated for 24 h at 50,000 cells/well in clear bottomed 96 well plates and were dye loaded for 60 min with 2 μM Fluo-4-AM in assay buffer. After cell washing, the plate was loaded on a fluorometric imaging plate reader (FLIPR), compound dilution series added to the cells, and the calcium signal recorded for 5 min in order to detect agonist activity. After 20 min of incubation with compound, a concentration natural agonist (oxytocin or AVP depending on the receptor) giving 80% of the maximum signal was added to the plate and the calcium signal recorded for 5 min in order to detect antagonist activity of the test compound.

The calcium signal reduction due to the antagonist activity of the compounds was fitted to a single site competition equation with variable slope and formula Y = Bottom + (Top-Bottom)/(1 + 10^((LogIC$_{50}$-X)∗HillSlope)), where Y is the% normalized fluorescence, Bottom is the minimum Y, Top is the maximum Y, IC_{50} is the concentration inhibiting 50% of the agonist induced fluorescence, X is the logarithm of the concentration of the competing compound, and Hillslope the Hill coefficient. All compounds were tested at least 3 times in duplicate

Acknowledgments

This work was supported by the EPSRC (EP/F500416/1 and EP/K503733/1), the Wellcome Trust and EPSRC Centre of Excellence in Medical Engineering (WT 088641/Z/09/Z), the Innovative Medicines Initiative Joint Undertaking under grant agreement (No. 115300), resources of which are composed of financial contribution from the European Union's Seventh Framework Programme (FP7/2007-2013) and EFPIA companies' in-kind contribution.

A. Supplementary data

Supplementary data associated with this article can be found, in the online version, at https://doi.org/10.1016/j.bmc.2018.03.019.

References

1. Van Dongen PW, Van Roosmalen J, De Boer CN, Van Rooij J. Oxytocics for the prevention of post-partum haemorrhages. A review. *Pharm Weekbl Sci*. 1991;13:238–243.
2. Maughan KL, Heim SW, Galazka SS. Preventing postpartum hemorrhage: managing the third stage of labor. *Am Fam Physician*. 2006;73:1025–1028.
3. Hawe A, Poole R, Romeijn S, Kasper P, van der Heijden R, Jiskoot W. Towards heat-stable oxytocin formulations: analysis of degradation kinetics and identification of degradation products. *Pharm Res*. 2009;26:1679–1688.
4. Hogan MC, Foreman KJ, Naghavi M, et al. Maternal mortality for 181 countries, 1980–2008: a systematic analysis of progress towards Millennium Development Goal 5. *Lancet*. 2010;375:1609–1623.
5. Khan KS, Wojdyla D, Say L, Gulmezoglu AM, Van Look PF. WHO analysis of causes of maternal death: a systematic review. *Lancet*. 2006;367:1066–1074.
6. Wisniewski K, Finnman J, Flipo M, Galyean R, Schteingart CD. On the mechanism of degradation of oxytocin and its analogues in aqueous solution. *Biopolymers*. 2013;100:408–421.
7. Gazis D. Plasma half-lives of vasopressin and oxytocin analogs after IV injection in rats. *Proc Soc Exp Biol Med*. 1978;158:663–665.
8. Chini B, Mouillac B, Ala Y, et al. Molecular basis for agonist selectivity in the vasopressin/oxytocin receptor family. *Adv Exp Med Biol*. 1995;395:321–328.
9. Chini B, Mouillac B, Ala Y, et al. Tyr115 is the key residue for determining agonist selectivity in the V1a vasopressin receptor. *EMBO J*. 1995;14:2176–2182.
10. Peter J, Burbach H, Adan RAH, et al. Molecular neurobiology and pharmacology of the Vasopressin/Oxytocin receptor family. *Cell Mol Neurobiol*. 1995;15:573–595.

11. Walter R, Schwartz IL, Darnell JH, Urry DW. Relation of the conformation of oxytocin to the biology of neurohypophyseal hormones. *Proc Nalt Acad Sci USA*. 1971;68:1355–1359.
12. Golubow J, Du Vigneaud V. Comparison of susceptibility of oxytocin and desamino-oxytocin to inactivation by leucine aminopeptidase and alpha-chymotrypsin. *Proc Soc Exp Biol Med*. 1963;112:218.
13. Chini B, Chinol M, Cassoni P, et al. Improved radiotracing of oxytocin receptor-expressing tumours using the new [111In]-DOTA-Lys8-deamino-vasotocin analogue. *Br J Cancer*. 2003;89:930–936.
14. Hunter DJ, Schulz P, Wassenaar W. Effect of carbetocin, a long-acting oxytocin analog on the postpartum uterus. *Clin Pharmacol Ther*. 1992;52:60–67.
15. Stymiest JL, Mitchell BF, Wong S, Vederas JC. Synthesis of oxytocin analogues with replacement of sulfur by carbon gives potent antagonists with increased stability. *JOC*. 2005;70:7799–7809.
16. Yamanaka T, Hase S, Sakakibara S, Schwartz IL, Dubois BM, Walter R. Crystalline Deamino-dicarba-oxytocin. Preparation and Some Pharmacological Properties. *Mol Pharmacol*. 1970;6:474–480.
17. Smith CW, Walter R, Moore S, Makofske RC, Meienhofer J. Synthesis and some biological properties of (cyclo-(1-L-aspartic acid,6-L-alpha, beta-diaminopropionic acid))oxytocin. *J Med Chem*. 1978;21:117–120.
18. de Araujo AD, Mobli M, Castro J, et al. Selenoether oxytocin analogues have analgesic properties in a mouse model of chronic abdominal pain. *Nat Commun*. 2014;5:1–12.
19. Muttenthaler M, Andersson A, de Araujo AD, Dekan Z, Lewis RJ, Alewood PF. Modulating oxytocin activity and plasma stability by disulfide bond engineering. *J Med Chem*. 2010;53:8585–8596.
20. Engstrom T, Barth T, Melin P, Vilhardt H. Oxytocin receptor binding and uterotonic activity of carbetocin and its metabolites following enzymatic degradation. *Eur J Pharmacol*. 1998;355:203–210.
21. Moertl MG, Friedrich S, Kraschl J, Wadsack C, Lang U, Schlembach D. Haemodynamic effects of carbetocin and oxytocin given as intravenous bolus on women undergoing caesarean delivery: a randomised trial. *BJOG*. 2011;118:1349–1356.
22. Passoni I, Leonzino M, Gigliucci V, Chini B, Busnelli M. Carbetocin is a functional selective gq agonist that does not promote oxytocin receptor recycling after inducing beta-arrestin-independent internalisation. *J Neuroendocrinol*. 2016;28:1–10.
23. Collins J, Tanaka J, Wilson P, et al. In situ conjugation of dithiophenol maleimide polymers and oxytocin for stable and reversible polymer-peptide conjugates. *Bioconjug Chem*. 2015;26:633–638.
24. Timmerman P, Beld J, Puijk WC, Meloen RH. Rapid and quantitative cyclization of multiple peptide loops onto synthetic scaffolds for structural mimicry of protein surfaces. *ChemBioChem*. 2005;6:821–824.
25. Jo H, Meinhardt N, Wu Y, et al. Development of alpha-helical calpain probes by mimicking a natural protein-protein interaction. *J Am Chem Soc*. 2012;134:17704–17713.
26. Angelini A, Morales-Sanfrutos J, Diderich P, Chen S, Heinis C. Bicyclization and tethering to albumin yields long-acting peptide antagonists. *J Med Chem*. 2012;55:10187–10197.
27. Werkhoven PR, van de Langemheen H, van der Wal S, Kruijtzer JA, Liskamp RM. Versatile convergent synthesis of a three peptide loop containing protein mimic of whooping cough pertactin by successive Cu(I)-catalyzed azide alkyne cycloaddition on an orthogonal alkyne functionalized TAC-scaffold. *J Pept Sci*. 2014;20:235–239.
28. Sharma KS, Durand G, Giusti F, et al. Glucose-based amphiphilic telomers designed to keep membrane proteins soluble in aqueous solutions: synthesis and physicochemical characterization. *Langmuir*. 2008;24:13581–13590.
29. Gimpl G, Fahrenholz F. The oxytocin receptor system: structure, function, and regulation. *Physiol Rev*. 2001;81:629–683.
30. Ratni H, Rogers-Evans M, Bissantz C, et al. Discovery of highly selective brain-penetrant vasopressin 1A antagonists for the potential treatment of autism via a chemogenomic and scaffold hopping approach. *J Med Chem*. 2015;58:2275–2289.
31. Meshykhi LS, Nel MR, Lucas DN. The role of carbetocin in the prevention and management of postpartum haemorrhage. *Int J Obstet Anesth*. 2016;28 (Supplement C).
32. Yamasue H. Promising evidence and remaining issues regarding the clinical application of oxytocin in autism spectrum disorders. *Psychiatry Clin Neurosci*. 2016;70:89–99.
33. Quintana DS, Westlye LT, Rustan ØG, et al. Low-dose oxytocin delivered intranasally with Breath Powered device affects social-cognitive behavior: a randomized four-way crossover trial with nasal cavity dimension assessment. *Transl Psychiatry*. 2015;5:1–9.

Please cite this article in press as: Beard R., et al. Bioorg. Med. Chem. (2018), https://doi.org/10.1016/j.bmc.2018.03.019